Advances in Nano Research, *Vol. 16, No. 3 (2024) 289-301*
https://doi.org/10.12989/anr.2024.16.3.289

Static bending response of axially randomly oriented functionally graded carbon nanotubes reinforced composite nanobeams

Ahmed Amine Daikh*[1,2], Ahmed Drai[3,4], Mohamed Ouejdi Belarbi[5,6], Mohammed Sid Ahmed Houari[2], Benoumer Aour[4], Mohamed A. Eltaher[7,8] and Norhan A. Mohamed[9]

[1]*Artificial Intelligence Laboratory for Mechanical and Civil Structures, and Soil, University Centre of Naama, Naama, Algeria*
[2]*Laboratoire d'Etude des Structures et de Mécanique des Matériaux, Département de Génie Civil, Faculté des Sciences et de la Technologie, Université Mustapha Stambouli B.P. 305, R.P. 29000 Mascara, Algérie*
[3]*Department of Mechanical Engineering, Mustapha STAMBOULI University of Mascara, 29000, Algeria*
[4]*LABAB Laboratory of ENPO, Oran, 31000, Algeria*
[5]*Laboratoire de Génie Energétique et Matériaux, LGEM, Université de Biskra, B.P. 145, R.P. 07000, Biskra, Algeria*
[6]*Department of Civil Engineering, Lebanese American University, Byblos, Lebanon*
[7]*Faculty of Engineering, Mechanical Engineering Department, King Abdulaziz University, P.O. Box 80204, Jeddah, Saudi Arabia*
[8]*Faculty of Engineering, Mechanical Design and Production Department, Zagazig University, Zagazig, Egypt*
[9]*Engineering Mathematics Department, Faculty of Engineering, Zagazig University, Zagazig Egypt*

(*Received May 22, 2021, Revised October 13, 2023, Accepted January 28, 2024*)

Abstract. In this work, an analytical model employing a new higher-order shear deformation beam theory is utilized to investigate the bending behavior of axially randomly oriented functionally graded carbon nanotubes reinforced composite nanobeams. A modified continuum nonlocal strain gradient theory is employed to incorporate both microstructural effects and geometric nano-scale length scales. The extended rule of mixture, along with molecular dynamics simulations, is used to assess the equivalent mechanical properties of functionally graded carbon nanotubes reinforced composite (FG-CNTRC) beams. Carbon nanotube reinforcements are randomly distributed axially along the length of the beam. The equilibrium equations, accompanied by nonclassical boundary conditions, are formulated, and Navier's procedure is used to solve the resulting differential equation, yielding the response of the nanobeam under various mechanical loadings, including uniform, linear, and sinusoidal loads. Numerical analysis is conducted to examine the influence of inhomogeneity parameters, geometric parameters, types of loading, as well as nonlocal and length scale parameters on the deflections and stresses of axially functionally graded carbon nanotubes reinforced composite (AFG CNTRC) nanobeams. The results indicate that, in contrast to the nonlocal parameter, the beam stiffness is increased by both the CNTs volume fraction and the length-scale parameter. The presented model is applicable for designing and analyzing microelectromechanical systems (MEMS) and nanoelectromechanical systems (NEMS) constructed from carbon nanotubes reinforced composite nanobeams.

Keywords: axially CNTs distribution; Navier's solution; nonlocal strain gradient higher order shear deformation theory; static bending and stress analyses

1. Introduction

Nowadays, carbon nanotubes (CNTs) have garnered significant attention and application in various scientific and technological domains. These cylindrical carbon structures, characterized by exceptional strength, electrical conductivity, and thermal properties, are composed of carbon atoms arranged in a hexagonal lattice, resembling a rolled-up sheet of graphene. CNTs come in two primary forms: single-walled (SWCNTs) with a single layer of carbon atoms and multi-walled (MWCNTs) with multiple concentric layers. Their unique structure and extraordinary properties have led to an array of applications across fields such as materials science, electronics, nanotechnology, and aerospace. As a result, CNTs remain at the forefront of cutting-edge research and innovation in the modern era. (Eltaher *et al*. 2016, 2020a, Mohamed *et al*. 2020, Wu *et al*. 2016, Daikh *et al*. 2021a).

Throughout the existing body of literature, numerous kinematic theories have been put forth to provide precise predictions of the mechanical responses exhibited by composite, sandwich, and functionally graded material (FGM) structures when subjected to a wide array of loading conditions. (Zenkour and Radwan 2020, Belarbi *et al*. 2020 a, b Belarbi *et al* 2016, Daikh and Zenkour 2020, Daikh *et al* 2020a, Ehyaei *et al*. 2016, Ebrahimi and Barati 2016, Bekhadda *et al*. 2019, Daikh *et al.* 2021b, Bensaid *et al*. 2019, Esen *et al*. 2021). One of the most straightforward and widely used theories is referred to as classical beam theory (CBT), which relies on the Euler-Bernoulli assumptions. However, it is important to note that CBT is solely suitable for the analysis of slender beams. (Ghannadpour *et al*. 2013, Najad *et al*. 2018). When dealing with moderately thick and thick beams, the classical beam theory (CBT) tends to underestimate deflection while overestimating buckling loads and natural frequencies, mainly due to its neglect of shear deformation effects. To

*Corresponding author, Ph.D.,
E-mail: aadaikh@cuniv-naama.dz

ISSN: 2287-237X (Print), 2287-2388 (Online)

address these limitations, shear deformation theories (SDT) have been introduced. The first-order shear deformation theory (FSDT), often known as the Timoshenko beam theory (TBT), was developed to account for transverse shear deformation effects. However, this theory requires a shear correction factor, which can be challenging to determine since it varies based on the geometries, material properties, and boundary conditions of each specific problem (Ferreira *et al*. 2009). To address the limitations of the first-order shear deformation theory (FSDT), researchers have devised several higher-order shear deformation theories (HSDT). These theories offer improved accuracy in representing the parabolic distribution of transverse shear stresses across the beam's thickness, all without the need for shear correction factors. Higher-order shear deformation theories achieve this by expanding the in-plane displacement field with higher-order variations in relation to the thickness coordinate and ensuring that shear stresses at the top and bottom surfaces of the beam are maintained at zero. (Daikh *et al*. 2020b, c, d, Vo *et al*. 2015, Nguyen *et al*. 2014, Thai *et al*. 2016, Daikh and Zenkour 2019a, b, Eltaher *et al*. 2016).

In the present era, engineering nanostructures like nanorods, nanobeams, and nanoplates have gained extensive use across a wide array of applications, primarily owing to their exceptional mechanical, thermal, chemical, and electronic properties. (Abdelrahman and Eltaher 2020, Houari *et al*. 2018). Nanostructures find extensive utility in MEMS/NEMS and nano actuators, where size effects play a prominent role. In these applications, it becomes imperative to account for the size effects of these nanostructures, which are often overlooked in classical continuum theories, to ensure precise and accurate design and analysis. To address this challenge, several non-classical continuum theories that incorporate additional material length scale parameters have been formulated. These include the nonlocal elasticity theory (Eringen 1972, 1983), strain gradient theory (Mindlin 1963), modified couple stress theory (MCST) (Yang *et al*. 2002), and nonlocal strain gradient theory (NSGT) (Askes and Aifantis 2009).

Axially functionally graded (AFG) materials represent a unique subset of functionally graded materials (FGMs) where the material gradient varies specifically along the length of the structures. In their work, Sarkar and Ganguli (2014) provided a precise solution for the free vibration response of a clamped AFG Timoshenko beam. Abo-Bakr *et al*. (2020) anticipated the optimal weight of AFG microbeams in terms of buckling and vibration behavior, employing the Modified Couple Timoshenko Beam Theory. Şimşek (2015) investigated the nonlinear free vibration behavior of AFG microbeams using the Modified Couple Stress Theory (MCST) and the Euler-Bernoulli Theory (EBT). Meanwhile, Shafiei *et al*. (2016) introduced a semi-analytical approach to explore the nonlinear vibration characteristics of AFG tapered microbeams. They utilized Eringen's nonlocal theory in conjunction with the Euler-Bernoulli Theory (EBT). Additionally, Li *et al*. (2017) delved into the buckling, bending, and free vibration behavior AFG nanobeams, employing both the Nonlocal Strain Gradient Theory (NSGT) and the Euler-Bernoulli Theory (EBT). Wang and Wu (2016) investigated the influence of thermal effects on the dynamic response of AFG beams subjected to a moving harmonic load. This study considered both the Euler-Bernoulli Theory (EBT) and the Timoshenko Beam Theory (TBT). Abo-Bakr *et al*. (2021) conducted a study using multi-objective shape optimization and Pareto analysis to explore the optimal weight of modified couple stress AFG nanobeams while considering both buckling and frequency constraints. Ebrahimi and Barati (2017) employed a Galerkin-based solution technique to investigate the buckling behavior of AFG nanobeams, with their analysis grounded in the Nonlocal Strain Gradient Theory (NSGT). Akgoz (2019) addressed the static buckling problem of AFG tapered micro-columns with varying boundary conditions. Rajasekaran and Bakhshi Khaniki (2019) presented a comprehensive study on the size-dependent mechanical behavior of AFG beams based on the Nonlocal Strain Gradient Theory (NSGT). They employed the finite element method for their analysis. Zheng *et al*. (2019) introduced a novel nonlinear finite element formulation based on the Modified Couple Stress Theory (MCST) and the Euler-Bernoulli Theory (EBT) to investigate the free vibration response of AFG tapered microbeams. Cao *et al*. (2018) carried out a free vibration analysis of AFG beams, utilizing the asymptotic development method. Wang *et al*. (2020) investigated the hygrothermal mechanical behavior of AFG microbeams. They employed a refined First-Order Shear Deformation Theory (FSDT) for their analysis Civalek *et al*. (2021) explored the free vibration behavior of microbeams made of carbon nanotubes reinforced composite (CNTRC) using various beam theories and the couple stress theory. They applied Navier's solution procedure for their investigation. Karamanli and Vo (2021) proposed a finite element model to study the mechanical response of composite beams reinforced with CNTs and graphene nanoplatelets. Their model considered the effect of thickness stretching. El-Ashmawy and Xu (2021**)** analyzed the influence of CNTs gradation distribution and orientation on the static and dynamic behavior of FG CNTRC beams. They employed the Timoshenko beam theory for their analysis.

The study of FG CNTs nanobeam bending is indispensable in the realm of nanotechnology as it not only unravels the intricate mechanical properties of these materials, enabling the design and engineering of flexible electronic devices, precision drug delivery systems, and environmental sensors but also empowers structural health monitoring in civil engineering, exemplifying its profound impact on both technological innovation and the development of sustainable solutions across various scientific and practical domains.

It is apparent from the previously discussed literature that there is a limited number of studies pertaining to axially functionally graded nanobeams. Additionally, there is a lack of published work addressing the static response of AFG randomly oriented carbon nanotube-reinforced composite (CNTRC) nanobeams using a modified HSDT. This study aims to bridge this gap.

In this paper, a modified nonlocal strain gradient theory,

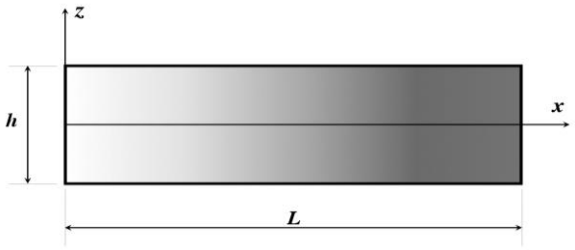

Fig. 1 Geometry of AFG-CNTRC beam

Table 1 Hill's elastic moduli for (10, 10) single-walled carbon nanotubes, Mehrabadi *et al*. (2012)

k_{cnt} [GPa]	l_{cnt}[GPa]	m_{cnt}[GPa]	n_{cnt}[GPa]	p_{cnt}[GPa]
271	88	17	1089	442

combined with a new HSDT, is employed to analyze the bending deflection and stresses in axially functionally graded carbon nanotubes reinforced composite (FG CNTRC) beams. These beams are subjected to various transverse loading profiles while taking into account factors such as the distribution of carbon nanotubes (CNTs), thickness ratio, nonlocal parameters, and length scale parameters. The governing equations are derived using the principle of total potential energy and are solved using Navier's procedure.

2. Problem formulation

Let's consider a straight AFG composite nanobeam with randomly oriented CNTs. This nanobeam has a length of "L" and a thickness represented by "h", as depicted in Fig. 1.

The beam is strengthened with carbon nanotubes (CNTs) that are randomly oriented. The percentage of CNTs in the volume varies and is distributed along the length of the beam. The analysis encompasses four different forms of CNT distribution: UD, FG-, FG-X, and FG-O;

$$\begin{aligned} V_{cnt} &= V_{cnt}^{*} \ \text{for UD distribution} \\ V_{cnt} &= \frac{2|2x-L|}{L}V_{cnt}^{*} \ \text{for FG}-\text{X distribution} \\ V_{cnt} &= 2-\frac{2|2x-L|}{L}V_{cnt}^{*} \ \text{for FG}-\text{O distribution} \\ V_{cnt} &= 1+\frac{|2x-L|}{L}V_{cnt}^{*} \ \text{for FG}-\text{V distribution} \end{aligned} \tag{1}$$

The effective Young's moduli and Poisson's ratio of the composite material, which is a mixture of carbon nanotubes (CNTs) and polymer, can be computed as outlined in the study by Abdelhaffez *et al*. (2023).

$$\begin{aligned} E_{ef}^{m} &= \frac{9KG}{3K+G} \\ \nu_{ef}^{m} &= \frac{3K-2G}{6K+2G} \end{aligned} \tag{2}$$

The Eshelby-Mori-Tanaka model, which builds upon the Mori-Tanaka concept of average stress in the matrix, was developed based on Eshelby's micromechanics theory, as discussed by Tornabene *et al*. (2019). In this model, carbon nanotubes (CNTs) can be treated as aggregated particles randomly distributed within the matrix. Unlike the rule of mixture, this model takes into account the agglomeration effect of CNTs, as emphasized by Kamarian *et al*. (2015). Consequently, the model provides expressions for the effective bulk modulus "K" and shear modulus "G".

$$\begin{aligned} K &= K_p + \frac{V_{cnt}\left(\delta_{cnt} - 3K_p\alpha_{cnt}\right)}{3\left(V_p + V_{cnt}\beta_{cnt}\right)} \\ G &= K_p + \frac{V_{cnt}\left(\eta_{cnt} - 2G_p\beta_{cnt}\right)}{2\left(V_p + V_{cnt}\beta_{cnt}\right)} \end{aligned} \tag{3}$$

The relationship between the volume fraction of polymer (V_p) and the volume fraction of carbon nanotubes (V_{cnt}) can be expressed as follows:

$$V_p = 1 - V_{cnt} \tag{4}$$

The parameters α_{cnt}, β_{cnt}, δ_{cnt} and η_{cnt}, which appear in the above relationships, can be determined or calculated as follows:

$$\alpha_{cnt} = \frac{3\left(K_p + G_p\right) + k_{cnt} - l_{cnt}}{3\left(G_p + k_{cnt}\right)} \tag{5}$$

$$\begin{aligned} \beta_{cnt} = \frac{1}{5}\Bigg(&\frac{4G_p + 2k_{cnt} + l_{cnt}}{3\left(G_p + k_{cnt}\right)} + \frac{4G_p}{G_p + p_{cnt}} \\ &+ \frac{2\left(G_p\left(3K_p + G_p\right) + G_p\left(3K_p + 7G_p\right)\right)}{G_p\left(3K_p + G_p\right) + m_{cnt}\left(3K_p + 7G_p\right)}\Bigg) \end{aligned} \tag{6}$$

$$\begin{aligned} \delta_{cnt} = \frac{1}{3}\Bigg(&n_{cnt} + 2l_{cnt} \\ &+ \frac{2(k_{cnt} + l_{cnt})\left(3K_p + 2G_p - l_{cnt}\right)}{G_p + k_{cnt}}\Bigg) \end{aligned} \tag{7}$$

$$\eta_{cnt} = \frac{1}{5}\begin{pmatrix} \frac{2}{3}(n_{cnt} - l_{cnt}) + \frac{8G_p p_{cnt}}{G_p + p_{cnt}} \\ + \frac{8m_{cnt}G_m\left(3K_p + 4G_p\right)}{3K_m\left(m_{cnt} + G_p\right) + G_p\left(7m_{cnt} + G_p\right)} \\ + \frac{2(k_{cnt} - l_{cnt})\left(2G_p + l_{cnt}\right)}{3\left(G_p + k_{cnt}\right)} \end{pmatrix} \tag{8}$$

Table 1 provides Hill's elastic moduli of (10, 10) SWCNTs for various chiral indices.

3. Equilibrium equations for Nanobeams

The displacement field of an AFG CNTRC nanobeam, as per the HSDT, can be described as follows (Daikh *et al*. 2019a):

$$\begin{aligned} u(x,z) &= u_0 - z\frac{\partial w_0}{\partial x} + f(z)\varphi_{\mathrm{x}} \\ w(x,z) &= w_0 \end{aligned} \tag{9}$$

In this context, u_u_0 and w_0 denote the displacements along the x- and z-directions, respectively, while φ_{x}

represents the rotation of the transverse normal with respect to the *x*-axis.

The shear deformation along the *z*-direction can be represented using a hyperbolic function as:

$$f(z) = h\sinh\left(\frac{z}{h}\right) - \frac{3z^3}{2h^2} \tag{10}$$

The kinematic strain components linked to the displacement field are articulated in the following manner:

$$\begin{aligned} \varepsilon_{xx} &= \varepsilon_{xx}^0 - z\varepsilon_{xx}^1 + f(z)\varepsilon_{xx}^2 \\ \gamma_{xz} &= \frac{df(z)}{dz}\varphi_x \end{aligned} \tag{11}$$

In this context, the strain components along the natural axis are characterized as:

$$\begin{aligned} \varepsilon_{xx}^0 &= \frac{\partial u}{\partial x} \\ \varepsilon_{xx}^1 &= \frac{\partial^2 w}{\partial x^2} \\ \varepsilon_{xx}^2 &= \frac{\partial \varphi_x}{\partial x} \end{aligned} \tag{12}$$

The relationships between stress and strain, known as the constitutive stress-strain relations, are expressed as:

$$\begin{Bmatrix} \sigma_{xx} \\ \sigma_{xz} \end{Bmatrix} = \begin{bmatrix} Q_{11} & 0 \\ 0 & Q_{55} \end{bmatrix} \begin{Bmatrix} \varepsilon_{xx} \\ \gamma_{xz} \end{Bmatrix} \tag{13}$$

where

$$Q_{11} = \frac{E_{11}}{1 - \nu_{12}\nu_{21}}, \quad Q_{55} = G_{12} \tag{14}$$

In this context, Q_{ij} represents the equivalent stiffness. The virtual strain energy of the beam can be written by:

$$\begin{aligned} \delta U &= \int_0^L \int_A (\sigma_{xx}\delta\varepsilon_{xx} + \sigma_{xz}\delta\gamma_{xz})\mathrm{d}A\mathrm{d}x \\ \delta U &= \int_0^L \begin{pmatrix} N_{xx}\dfrac{d\delta u}{\partial x} - M_{xx}\dfrac{d^2\delta w}{\partial x^2} \\ +P_{xx}\dfrac{d\delta\varphi_x}{\partial x} + Q_{xz}\delta\varphi_x \end{pmatrix} \mathrm{d}x\mathrm{d}z \end{aligned} \tag{15}$$

The virtual potential energy of the transverse load $q(x)$ is given by

$$\delta V = -\int_0^L q(\delta w)\mathrm{d}x \tag{16}$$

q(*x*) represents the applied transverse load. It's evident that the stress resultants in the current CNTRC nanobeam are connected to the strains through the following equations:

$$\begin{aligned} \begin{Bmatrix} N_{xx} \\ M_{xx} \\ P_{xx} \end{Bmatrix} &= \int_{-h/2}^{h/2} \begin{Bmatrix} 1 \\ z \\ f(z) \end{Bmatrix} \sigma_{xx}\,\mathrm{d}z \\ Q_{xz} &= \int_{-h/2}^{h/2} \frac{df(z)}{dz}\,\sigma_{xz}\,\mathrm{d}z \end{aligned} \tag{17}$$

It's important to highlight that the force and moment resultants of the CNTRC beam can be connected to the overall strains through the following relationship:

$$\begin{aligned} \begin{Bmatrix} N_{xx} \\ M_{xx} \\ P_{xx} \end{Bmatrix} &= \begin{bmatrix} A_{11} & B_{11} & C_{11} \\ B_{11} & D_{11} & F_{11} \\ C_{11} & F_{11} & H_{11} \end{bmatrix} \begin{Bmatrix} \varepsilon_x^0 \\ \varepsilon_x^1 \\ \varepsilon_x^2 \end{Bmatrix} \\ Q_{xz} &= A_{55}\gamma_{xz} \end{aligned} \tag{18}$$

where

$$\begin{aligned} &\{A_{11}, B_{11}, D_{11}, C_{11}, F_{11}, H_{11}\} \\ &= \int_{-h/2}^{h/2} Q_{11}\{1, z, z^2, f(z), zf(z), f(z)^2\}dz \end{aligned} \tag{19}$$

$$A_{55} = \int_{-h/2}^{h/2} Q_{55}\left[\frac{df(z)}{dz}\right]^2 dz \tag{20}$$

It is also worth noting that we can define the force and moment resultants within the displacement fields as follows:

$$\begin{aligned} N_{xx} &= A_{11}\frac{\partial u_0}{\partial x} - B_{11}\frac{\partial^2 w_0}{\partial x^2} + C_{11}\frac{\partial \varphi_x}{\partial x} \\ M_{xx} &= B_{11}\frac{\partial u_0}{\partial x} - D_{11}\frac{\partial^2 w_0}{\partial x^2} + F_{11}\frac{\partial \varphi_x}{\partial x} \\ P_{xx} &= C_{11}\frac{\partial u_0}{\partial x} - F_{11}\frac{\partial^2 w_0}{\partial x^2} + H_{11}\frac{\partial \varphi_x}{\partial x} \\ Q_{xz} &= A_{55}\varphi_x \end{aligned} \tag{21}$$

By using the principle of total potential energy, the following weak statement is obtained:

$$0 = \int_0^L \begin{pmatrix} N_{xx}\dfrac{d\delta u}{\partial x} - M_{xx}\dfrac{d^2\delta w}{\partial x^2} \\ +P_{xx}\dfrac{d\delta\varphi_x}{\partial x} + Q_{xz}\delta\varphi_x \end{pmatrix} \mathrm{d}x\mathrm{d}z - \int_0^L q(\delta w)\mathrm{d}x \tag{22}$$

Since the total virtual work done equals zero and the coefficients of δu, δw and $\delta\varphi_x$ are zero in $0 < x < L$, one can obtain the following governing equations,

$$\begin{aligned} \frac{\partial N_{xx}}{\partial x} &= 0 \\ \frac{\partial^2 M_{xx}}{\partial x^2} - q &= 0 \\ \frac{\partial P_{xx}}{\partial x} - Q_{xz} &= 0 \end{aligned} \tag{23}$$

4. Nonlocal strain gradient theory laminated nanobeam

This study combines the physical influence of strain gradient stress with nonlocal elastic stress fields and introduces a function of stresses, as proposed by Lim *et al.* (2015):

$$\sigma_{ij} = \sigma_{ij}^{(0)} - \frac{d\sigma_{ij}^{(1)}}{dx} \tag{24}$$

In this context, $\sigma_{ij}^{(0)}$ represents the classical stress corresponding to the strain ε_{kl}, while $\sigma_{ij}^{(1)}$ pertains to the higher-order stress corresponding to the strain gradient $\varepsilon_{kl,x}$. Furthermore, their specific expressions can be represented as:

$$\begin{aligned}\sigma_{ij}^{(0)} &= \int_0^L C_{ijkl}\alpha_0(x,x',e_0a)\varepsilon_{kl,x}(x')dx' \\ \sigma_{ij}^{(1)} &= l^2\int_0^L C_{ijkl}\alpha_1(x,x',e_1a)\varepsilon_{kl,x}(x')dx'\end{aligned} \tag{25}$$

In this case; C_{ijkl} is an elastic constant and l is the material length scale parameter introduced to consider the significance of the strain gradient stress field. e_0a and e_1a are the nonlocal parameters introduced to consider the significance of the nonlocal elastic stress field. Based on nonlocal kernel functions $\alpha_0(x,x',e_0a)$ and $\alpha_1(x,x',e_1a)$, the general constitutive relation of nonlocal strain constitutive relation can be written as, Eringen (1983):

C_{ijkl} represents the elastic constants, and "l" is the material length scale parameter introduced to account for the influence of the strain gradient stress field. "e_0a" and "e_1a" are nonlocal parameters introduced to consider the significance of the nonlocal elastic stress field. Utilizing nonlocal kernel functions$\alpha_0(x,x',e_0a)$ and $\alpha_1(x,x',e_1a)$, the general constitutive relation for the nonlocal strain can be expressed as outlined by Eringen (1983):

$$\begin{aligned}&[1-(e_1a)^2\nabla^2][1-(e_0a)^2\nabla^2]\sigma_{ij} \\ &= C_{ijkl}[1-(e_1a)^2\nabla^2]\varepsilon_{kl} - C_{ijkl}l^2[1-(e_0a)^2\nabla^2]\nabla^2\varepsilon_{kl}\end{aligned} \tag{26}$$

In this study, we assume that $e = e_0 = e_1$. ∇^2 represents the Laplacian operator. The overall nonlocal strain gradient constitutive relation can be described as follows (Daikh and Zenkour 2020):

$$[1-\mu\nabla^2]\sigma_{ij} = C_{ijkl}[1-\lambda\nabla^2]\varepsilon_{kl} \tag{27}$$

where $\mu = (ea)^2$ and $\lambda = l^2$.

$$(1-(e_0a)^2\nabla^2)\sigma_{ij} = C_{ijkl}(1-l^2\nabla^2)\varepsilon_{kl} \tag{28}$$

Hence, Daikh and Zenkour (2020) employed the constitutive relations for a nonlocal shear deformable axially carbon nanotubes reinforced composite (CNTRC) laminated nanobeam as follows

$$\sigma_{xx} - \mu\frac{\partial^2\sigma_{xx}}{\partial x^2} = \bar{Q}_{11}^k\left(\varepsilon_{xx} - \lambda\frac{\partial^2\varepsilon_{xx}}{\partial x^2}\right) \tag{29}$$

$$\sigma_{xz} - \mu\frac{\partial^2\sigma_{xx}}{\partial x^2} = \bar{Q}_{55}^k\left(\gamma_{xz} - \lambda\frac{\partial^2\gamma_{xz}}{\partial x^2}\right) \tag{30}$$

By incorporating equations (29) and (30) into equation (21), we can derive the relationship for stress resultants.

$$\begin{aligned}N_{xx} - \mu\frac{\partial^2N_{xx}}{\partial x^2} &= \left(1-\lambda^2\frac{\partial^2}{\partial x^2}\right)\left[A_{11}\frac{\partial u_0}{\partial x} - B_{11}\frac{\partial^2w_0}{\partial x^2} + C_{11}\frac{\partial\varphi_x}{\partial x}\right] \\ M_{xx} - \mu\frac{\partial^2M_{xx}}{\partial x^2} &= \left(1-\lambda^2\frac{\partial^2}{\partial x^2}\right)\left[B_{11}\frac{\partial u_0}{\partial x} - D_{11}\frac{\partial^2w_0}{\partial x^2} + F_{11}\frac{\partial\varphi_x}{\partial x}\right] \\ P_{xx} - \mu\frac{\partial^2P_{xx}}{\partial x^2} &= \left(1-\lambda^2\frac{\partial^2}{\partial x^2}\right)\left[C_{11}\frac{\partial u_0}{\partial x} - F_{11}\frac{\partial^2w_0}{\partial x^2} + H_{11}\frac{\partial\varphi_x}{\partial x}\right] \\ Q_{xz} - \mu\frac{\partial^2Q_{xz}}{\partial x^2} &= \left(1-\lambda\frac{\partial^2}{\partial x^2}\right)[A_{55}\varphi_x]\end{aligned} \tag{31}$$

By substituting the equations (31), which pertain to the force and moment resultants, into the governing equations represented by equation (23), the governing equations for an axially functionally graded (AFG) carbon nanotubes reinforced composite (CNTRC) nanobeam, considering nonlocal strain gradient effects, can be expressed as follows:

$$\begin{aligned}&\left(1-\lambda\frac{\partial^2}{\partial x^2}\right)\left(A_{11}\frac{\partial^2u_0}{\partial x^2} - B_{11}\frac{\partial^3w_0}{\partial x^3} + C_{11}\frac{\partial^2\varphi_x}{\partial x^2}\right) = 0 \\ &\left(1-\lambda\frac{\partial^2}{\partial x^2}\right)\begin{pmatrix}B_{11}\dfrac{\partial^3u_0}{\partial x^3} \\ -D_{11}\dfrac{\partial^4w_0}{\partial x^4} + F_{11}\dfrac{\partial^3\varphi_x}{\partial x^3}\end{pmatrix} - \left(1-\mu\frac{\partial^2}{\partial x^2}\right)q = 0 \\ &\left(1-\lambda\frac{\partial^2}{\partial x^2}\right)\left(C_{11}\frac{\partial^2u_0}{\partial x^2} - F_{11}\frac{\partial^3w_0}{\partial x^3} + H_{11}\frac{\partial^2\varphi_x}{\partial x^2} - J_{66}\varphi_x^1\right) = 0\end{aligned} \tag{32}$$

5. Exact solutions for FG-CNTRC nanobeams

The functions of the displacement field that meet the boundary conditions for simply-supported and simply-supported cross-ply laminated beams can be expressed as follows (Daikh *et al*. 2019b):

$$\begin{aligned}u_0 &= \sum_{m=1}^{\infty} U_m\cos(\beta x) \\ w_0 &= \sum_{m=1}^{\infty} W_m\sin(\beta x) \\ \varphi_x &= \sum_{m=1}^{\infty} X_m\cos(\beta x)\end{aligned} \tag{33}$$

Here, U_{mn}, V_{mn} and X_{mn} are arbitrary parameters, and $\beta = m\pi/L$. When we substitute Eq. (33) into Eq. (32), it yields the system stiffness matrix as follows:

$$\begin{bmatrix}-A_{11}(\beta^2+\lambda\beta^4) & B_{11}(\beta^3+\lambda\beta^5) & -C_{11}(\beta^2+\lambda\beta^4) \\ 0 & -D_{11}(\beta^4+\lambda\beta^6) & F_{11}(\beta^3+\lambda\beta^5) \\ symmetric & 0 & -H_{11}(\beta^2+\lambda\beta^4)-A_{55}(1+\lambda\beta^2)\end{bmatrix}$$
$$\begin{Bmatrix}U_m \\ W_m \\ X_m\end{Bmatrix} = \begin{Bmatrix}0 \\ (1+\mu\beta^2)Qm \\ 0\end{Bmatrix} \tag{34}$$

6. Transverse applied loads

The first example of transverse loading is a uniform one, where the load is applied uniformly to the top surface of the nanobeam, specifically at $z = h/2$. The expression for this load can be given as follows:

$$q(x) = \sum_{m=1}^{\infty} Q_m\sin(\beta x) \tag{35}$$

The coefficients of the Fourier expansion can be expressed as follows:

$$\begin{aligned}Q_m &= \frac{4q_0}{m\pi} \quad \text{for } m = 1,3,5,\ldots \\ Q_m &= 0 \quad \text{for } m = 2,4,6,\ldots\end{aligned} \tag{36}$$

The second type of loading exhibits a sinusoidal distribution, as depicted in Fig. 2. The mathematical

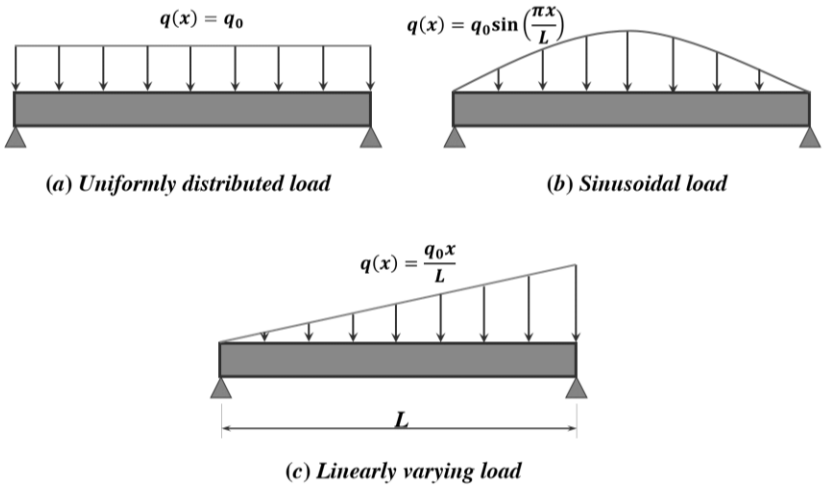

Fig. 2 Types of loads applied in the beam formulation

Table 2 Nondimensional deflection and stresses in uniformly distributed CNTRC beam

V_{cnt}^*	L/h	$\bar{w}$		$\bar{\sigma}_{xx}$		$\bar{\tau}_{xz}$	
		TSDT [86]	Present	TSDT [86]	Present	TSDT [86]	Present
Uniform load							
0,12%	10	0.704	7.0377	8.399	8.3982	0.701	0.7008
	15	0.524	0.5237	11.849	11.8488	0.716	0.7171
	20	0.461	0.4605	15.448	15.4491	0.725	0.7253
Sinusoidal load							
0,12%	10	0.562	0.5616	6.970	6.9681	0.472	0.4724
	15	0.416	0.4163	9.716	9.7149	0.475	0.4751
	20	0.365	0.3650	12.608	12.6065	0.476	0.4761

representation of this load can be expressed as:

$$q(x) = \sum_{m=1}^{\infty} q_0 \sin(\beta x) \tag{37}$$

The third type of loading involves linearly varying loads, can be described by the following expression:

$$\begin{gathered} q(x) = \frac{q_0 x}{L} \\ Q_m = -\frac{2q_0}{m\pi}\cos(m\pi) \quad \text{for } m = 1,3,5,\ldots \\ Q_m = 0 \quad \text{for } m = 2,4,6,\ldots \end{gathered} \tag{38}$$

7. Numerical results

The primary objective of this study is to investigate the bending deflection and stress distribution in randomly oriented AFG CNTRC nanobeams using a hyperbolic HSDT. The nanobeam in question is considered to be simply supported at both ends. The material composition of the nanobeam consists of a polymer matrix reinforced with Armchair (10,10) single-walled carbon nanotubes (SWCNTs). The mechanical properties of the matrix are $E_p = 2.5$ GPa and $\upsilon_p = 0.19$. To present the numerical results in terms of dimensionless deflection and stress parameters, the following formulas are employed:

$$\bar{w} = \frac{10^2 E_p h^2}{L^4 q_0} w\left(\frac{L}{2}\right) \tag{39}$$

$$\bar{\sigma}_{xx} = -\frac{h}{L q_0}\sigma_{xx}\left(\frac{L}{2}, \frac{h}{2}\right) \tag{40}$$

$$\bar{\tau}_{xz} = \frac{h}{L q_0}\tau_{xz}(0,0) \tag{41}$$

A comparative study is conducted in Table 2 to validate the accuracy of the applied inverse trigonometric higher-order shear deformation theory (HSDT) with the results obtained by Wattanasakulpong and Ungbhakorn (2013) using the Third-Order Shear Deformation Theory (TSDT) proposed by Reddy. The results presented in Table 2 demonstrate that the proposed theory aligns well and closely with the results obtained by Wattanasakulpong and Ungbhakorn (2013).

Table 3 provides an overview of how the volume fraction of CNTs impacts the dimensionless central deflection of an AFG CNTRC beam when subjected to various transverse loads. The CNTs volume fraction is systematically varied from 0 to 1, where a value of $V_{cnt}^* = 0$ signifies a fully polymer nanobeam. A similar analysis is conducted in Tables 4 and 5, focusing on the axial stresses

Table 3 Effect of CNTs volume fraction on the dimensionless central deflection of axially FG-X CNTRC beam

$V_{cnt}^{*}(\%)$	Sinusoidal load			Uniform load			Linear load		
	L/*h*=5	*L*/*h* =10	*L*/*h* =20	*L*/*h*=5	*L*/*h* =10	*L*/*h* =20	*L*/*h*=5	*L*/*h* =10	*L*/*h* =20
0.0	1.3611	1.2642	1.2400	1.7219	1.6024	1.5725	1.7219	1.6024	1.5725
0.2	1.2151	1.1286	1.1070	1.5372	1.4305	1.4038	1.5372	1.4305	1.4038
0.4	1.0974	1.0193	0.9997	1.3882	1.2919	1.2677	1.3882	1.2919	1.2677
0.6	1.0003	0.9291	0.9113	1.2655	1.1776	1.1557	1.2655	1.1777	1.1557
0.8	0.9190	0.8536	0.8373	1.1626	1.0819	1.0617	1.1627	1.0820	1.0618
1.0	0.8499	0.7894	0.7743	1.0752	1.0006	0.9819	1.0752	1.0006	0.9819

Table 4 Effect of CNTs volume fraction on the dimensionless axial stress of axially FG-X CNTRC beam

$V_{cnt}^{*}(\%)$	Sinusoidal load			Uniform load			Linear load		
	L/*h*=5	*L*/*h* =10	*L*/*h* =20	*L*/*h*=5	*L*/*h* =10	*L*/*h* =20	*L*/*h*=5	*L*/*h* =10	*L*/*h* =20
0.0	3.0926	6.1058	12.1718	3.8031	7.5265	15.0133	0.9508	1.8816	3.7533
0.2	2.7609	5.4508	10.8662	3.3951	6.7192	13.4028	0.8488	1.6798	3.3507
0.4	2.4933	4.9225	9.8130	3.0660	6.0679	12.1037	0.7665	1.5170	3.0259
0.6	2.2729	4.4873	8.9454	2.7950	5.5314	11.0336	0.6987	1.3829	2.7584
0.8	2.0881	4.1226	8.2184	2.5678	5.0819	10.1369	0.6420	1.2705	2.5342
1.0	1.9311	3.8126	7.6003	2.3747	4.6997	9.3745	0.5937	1.1749	2.3436

Table 5 Effect of CNTs volume fraction on the dimensionless shear stress of axially FG-X CNTRC beam.

$V_{cnt}^{*}(\%)$	Sinusoidal load			Uniform load			Linear load		
	L/*h*=5	*L*/*h* =10	*L*/*h* =20	*L*/*h*=5	*L*/*h* =10	*L*/*h* =20	*L*/*h*=5	*L*/*h* =10	*L*/*h* =20
0.0	0.4767	0.4772	0.4773	0.7329	0.7413	0.7454	-0.3665	-0.3707	-0.3727
0.2	0.5279	0.5284	0.5285	0.8116	0.8209	0.8254	-0.4058	-0.4104	-0.4127
0.4	0.5691	0.5697	0.5698	0.8750	0.8850	0.8899	-0.4375	-0.4425	-0.4450
0.6	0.6031	0.6037	0.6038	0.9273	0.9379	0.9431	-0.4636	-0.4689	-0.4715
0.8	0.6316	0.6322	0.6324	0.9711	0.9822	0.9876	-0.4855	-0.4911	-0.4938
1.0	0.6559	0.6565	0.6566	1.0083	1.0199	1.0255	-0.5042	-0.5099	-0.5128

Table 6 Effect of CNTs distribution patterns on the dimensionless axial stress of axially CNTRC beam.

Patterns	*L*/*h*	$V_{cnt}^{*}(\%)$					
		0.0	0.2	0.4	0.6	0.8	1.0
UD	5	3.0926	3.0926	3.0926	3.0926	3.0926	3.0926
	10	6.1058	6.1058	6.1058	6.1058	6.1058	6.1058
	20	12.1718	12.1718	12.1718	12.1718	12.1718	12.1718
FG-X	5	3.0926	2.7609	2.4933	2.2729	2.0881	1.9311
	10	6.1058	5.4508	4.9225	4.4873	4.1226	3.8126
	20	12.1718	10.8662	9.8130	8.9454	8.2184	7.6003
FG-O	5	3.0926	3.4244	3.6921	3.9126	4.0974	4.2546
	10	6.1058	6.7608	7.2893	7.7246	8.0896	8.3999
	20	12.1718	13.4775	14.5310	15.3990	16.1265	16.7451
FG-V	5	3.0926	3.0926	3.0926	3.0926	3.0926	3.0925
	10	6.1058	6.1058	6.1058	6.1057	6.1056	6.1056
	20	12.1718	12.1718	12.1717	12.1716	12.1715	12.1714

and shear stresses. These tables collectively demonstrate the influence of CNTs volume fraction on the behavior of the beam under different loading conditions.

Tables 6 and 7 provide insights into the impact of both

Table 7 Effect of CNTs distribution patterns on the dimensionless shear stress of axially CNTRC beam

Patterns	L/h	$V_{cnt}^{*}(\%)$					
		0.0	0.2	0.4	0.6	0.8	1.0
UD	5	0.4767	0.4767	0.4767	0.4767	0.4767	0.4767
	10	0.4772	0.4772	0.4772	0.4772	0.4772	0.4772
	20	0.4773	0.4773	0.4773	0.4773	0.4773	0.4773
FG-X	5	0.4767	0.5279	0.5691	0.6031	0.6316	0.6559
	10	0.4772	0.5284	0.5697	0.6037	0.6322	0.6565
	20	0.4773	0.5285	0.5698	0.6038	0.6324	0.6566
FG-O	5	0.4767	0.4256	0.3843	0.3504	0.3219	0.2977
	10	0.4772	0.4260	0.3847	0.3507	0.3222	0.2980
	20	0.4773	0.4261	0.3848	0.3508	0.3223	0.2980
FG-V	5	0.4767	0.5279	0.5691	0.6031	0.6316	0.6559
	10	0.4772	0.5284	0.5697	0.6037	0.6322	0.6565
	20	0.4773	0.5285	0.5698	0.6038	0.6324	0.6566

Table 8 Effect of nonlocal and length scale parameters on the dimensionless central deflection of axially CNTRC beam

μ	λ	$V_{cnt}^{*}(\%)$					
		0.0	0.2	0.4	0.6	0.8	1.0
0.0	0.0	1.2642	1.1286	1.0192	0.9291	0.8536	0.7894
	0.5	1.2048	1.0756	0.9713	0.8854	0.8135	0.7523
	1.0	1.1507	1.0273	0.9277	0.8457	0.7769	0.7185
	1.5	1.1012	0.9831	0.8878	0.8093	0.7435	0.6876
	2.0	1.0558	0.9426	0.8512	0.7760	0.7129	0.6593
0.5	0.0	1.3266	1.1843	1.0695	0.9750	0.8957	0.8284
	0.5	1.2642	1.1286	1.0192	0.9291	0.8536	0.7894
	1.0	1.2075	1.0779	0.9735	0.8874	0.8153	0.7540
	1.5	1.1556	1.0316	0.9316	0.8493	0.7802	0.7216
	2.0	1.1079	0.9891	0.8932	0.8143	0.7481	0.6918
1.0	0.0	1.3890	1.2400	1.1198	1.0208	0.9379	0.8673
	0.5	1.3237	1.1817	1.0672	0.9728	0.8938	0.8265
	1.0	1.2642	1.1286	1.0192	0.9291	0.8536	0.7894
	1.5	1.2099	1.0801	0.9754	0.8892	0.8169	0.7555
	2.0	1.1600	1.0356	0.9352	0.8525	0.7833	0.7244
1.5	0.0	1.4514	1.2957	1.1701	1.0667	0.9800	0.9063
	0.5	1.3832	1.2348	1.1151	1.0165	0.9339	0.8637
	1.0	1.3210	1.1793	1.0650	0.9709	0.8920	0.8249
	1.5	1.2642	1.1286	1.0192	0.9291	0.8536	0.7894
	2.0	1.2121	1.0821	0.9772	0.8908	0.8184	0.7569
2.0	0.0	1.5138	1.3514	1.2204	1.1125	1.0221	0.9452
	0.5	1.4426	1.2879	1.1630	1.0602	0.9740	0.9008
	1.0	1.3778	1.2300	1.1108	1.0126	0.9303	0.8603
	1.5	1.3186	1.1772	1.0631	0.9691	0.8903	0.8234
	2.0	1.2642	1.1286	1.0192	0.9291	0.8536	0.7894

carbon nanotubes distribution patterns, CNTs volume fraction, and thickness ratio on the dimensionless axial stresses and shear stresses of randomly AFG CNTRC beams, respectively. These tables highlight that the stresses, both axial and shear, are notably influenced by the distribution of CNTs and their volume fraction. The choice

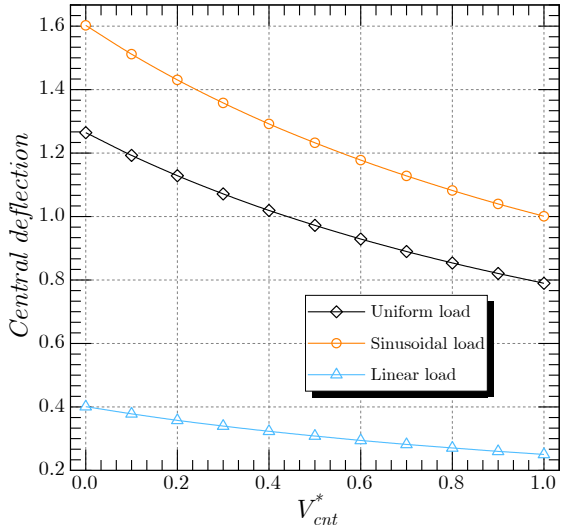

Fig. 3 Effect of CNTs volume fraction on the central deflection for various loading types ($FG-X$, L/h =10,$\mu=\lambda=0$)

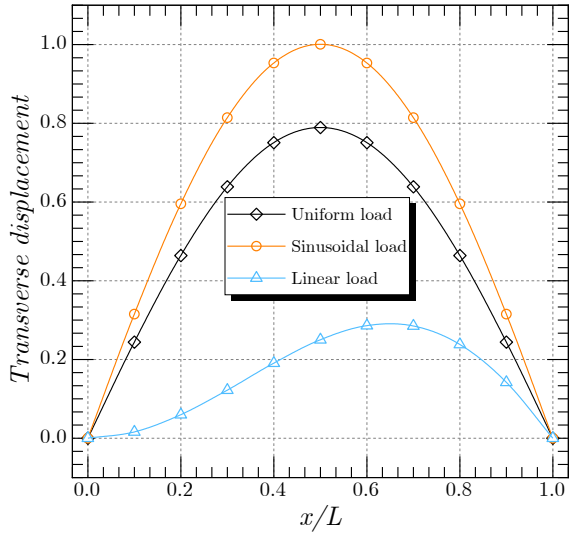

Fig. 4 Effect of the loading type on the transverse displacement ($FG-X$, L/h =10,$\mu=\lambda=0$)

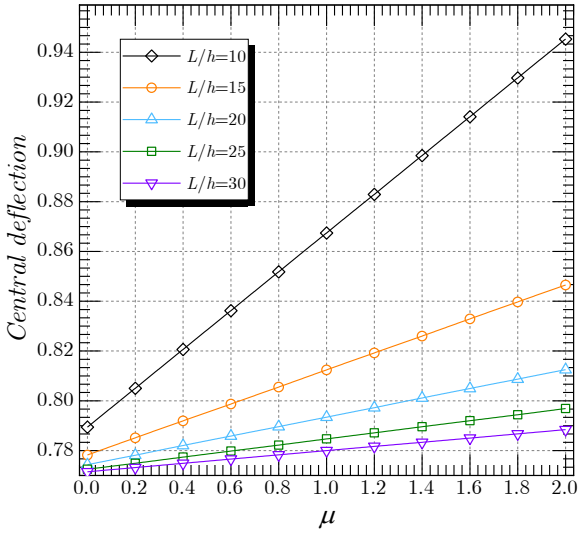

Fig. 5 Central deflection versus the nonlocal parameter "μ" and thickness ratio L/h ($FG-X, p=V^*_{cnt}$=1%, $\lambda=0$).

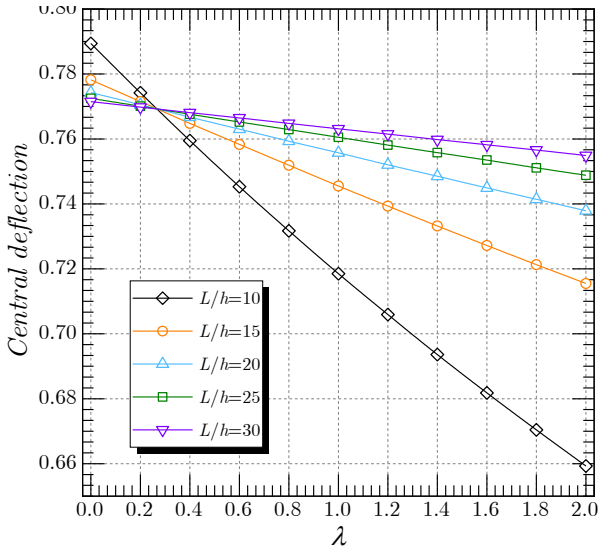

Fig. 6 Central deflection versus the length scale parameter "λ" and thickness ratio L/h ($FG-X, p=V^*_{cnt}=1\%$, $\mu=0$)

of CNTs distribution and the volume fraction significantly affects the stress distribution within the beam.

Table 8 explores the impact of the nonlocal parameter μ and the length scale parameter λ on the central deflection while considering various values of the CNTs volume fraction. The parameters μ and λ are systematically varied from 0 to 2, while the CNTs volume fraction $V^*_{cnt}(\%)$ ranges from 0% to 1%. The table demonstrates that as the volume fraction of CNTs increases, the stiffness of the nanobeam also increases, leading to a decrease in deflection. Additionally, it is observed that the nonlocal size effect, represented by μ, tends to soften the structure, resulting in an increase in deflection as μ increases. Conversely, the microstructure parameter λ tends to strengthen the structure, causing a reduction in deflection as λ increases. These findings emphasize the interplay of CNTs volume fraction, nonlocal parameters, and length scale parameters in influencing the behavior of the nanobeam.

Fig. 5 demonstrates the influence of the nonlocal parameter μ for various thickness ratio values on the central deflection. It is evident that as the nonlocal parameter μ increases, the central deflection consistently increases, irrespective of the thickness ratio. Additionally, increasing the thickness ratio results in a decreased central deflection of the AFG CNTRC beam. This figure clearly illustrates that the stiffness of the beam is reduced with an increase in the nonlocal parameter μ.

Fig. 6 demonstrates the influence of the length scale parameter λ on the central deflection for various thickness ratios. Unlike the nonlocal parameter effect, it is observed that as the length scale parameter λ increases, the stiffness of the beam increases, resulting in a decrease in the central deflection. This figure highlights the impact of the length scale parameter on beam stiffness and, consequently, its effect on the central deflection.

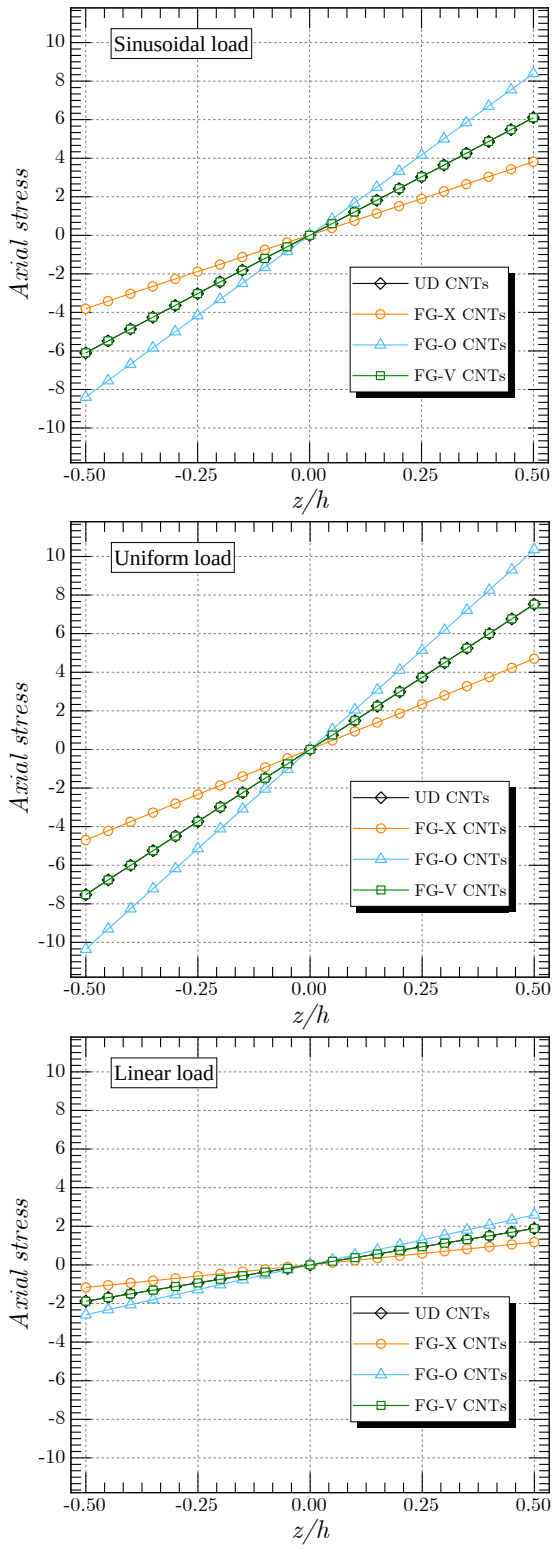

Fig. 7 Effect of CNTs distribution patterns on the axial stresses ($V_{cnt}^{*} = 1\%,\ p = 1,\ L/h = 10,\ \mu = \lambda = 0$)

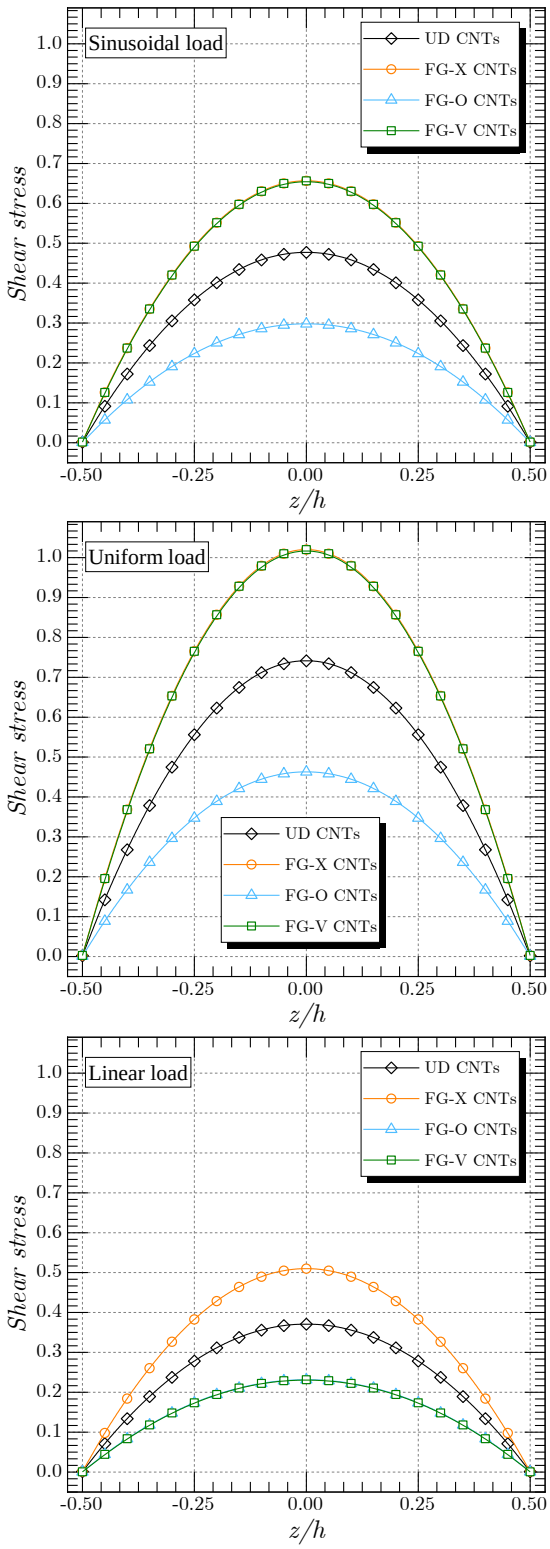

Fig. 8 Effect of CNTs distribution patterns on the shear stresses ($V_{cnt}^{*} = 1\%,\ p = 1,\ L/h = 10,\ \mu = \lambda = 0$).

Fig. 7 depicts the impact of carbon nanotubes distribution patterns on the axial stresses of randomly oriented AFG CNTRC beams subjected to various transverse loadings. This figure provides insights into how different CNTs distribution patterns influence the axial stresses under different loading conditions. It is evident from the figure that the axial stresses exhibit tensile forces at the top surface and compressive forces at the bottom surface of the beams. This distribution of stresses corresponds to a typical behavior observed in such structures. For the case of uniform loads, it's notable that the axial stresses are more concentrated at the midpoint of the beam ($x = L/2$). This

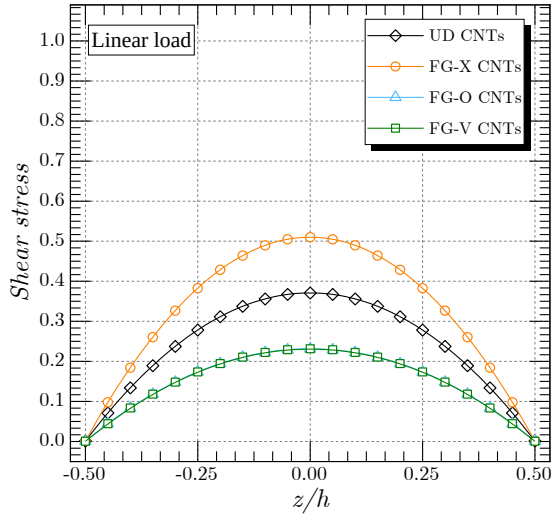

Fig. 8 Effect of CNTs distribution patterns on the shear stresses ($V^*_{cnt} = 1\%,\ p = 1,\ L/h = 10,\ \mu = \lambda = 0$)

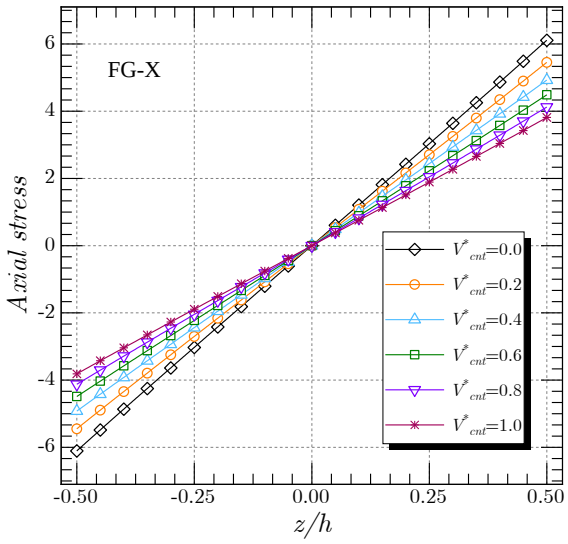

Fig. 9 Effect of CNTs volume fraction on the axial stresses ($FG-X,\quad L/h = 10,\ \mu = \lambda = 0$)

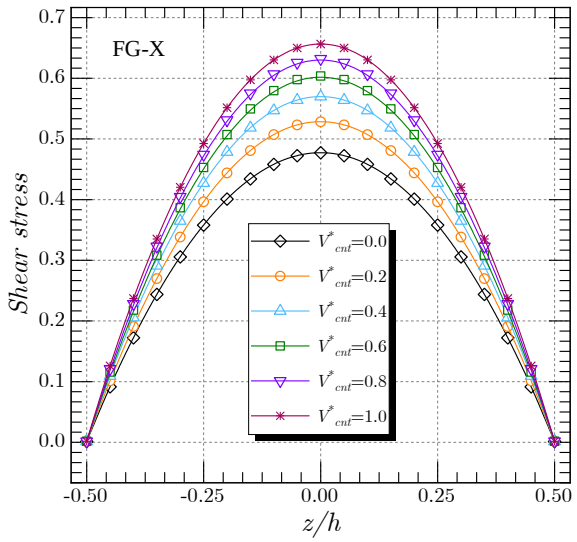

Fig. 10 Effect of CNTs volume fraction on the shear stresses ($FG-X,\quad L/h = 10,\ \mu = \lambda = 0$)

concentration of stresses occurs at the center of the beam due to the uniform load distribution.

In Fig. 8, the impact of carbon nanotubes distribution patterns on the shear stresses of randomly oriented AFG CNTRC beams subjected to various transverse loadings is depicted. The maximum stress results occur at a point on the midplane of the beam. This means that the highest stresses are experienced at the central section of the beam, along its midplane.

Figs. 9 and 10 display the impact of the CNTs volume fraction on the axial stresses and shear stresses of AFG CNTRC beams. These figures provide a visual representation of how varying CNTs volume fraction influences both axial and shear stresses within the beams. It is evident from these figures that the CNTs volume fraction exerts a significant influence on both axial and shear stresses. The variation in CNTs volume fraction leads to notable changes in the distribution of these stresses within the beams.

8. Conclusions

In this research, a comprehensive investigation was conducted for the first time on the stresses and deflection of randomly oriented axially functionally graded carbon nanotubes reinforced composite (CNTRC) beams. The displacement field was formulated based on a novel higher shear deformation theory. By incorporating nonlocal strain gradient theory and employing the principle of total potential energy, the equilibrium equations were derived and subsequently solved using Navier's method. Three distinct types of loads were taken into account. The numerical examples have revealed the following key findings:

• The stiffness of the AFG CNTRC beam rises with an increase in the volume fraction of carbon nanotubes.

• Incorporating the nonlocal parameter results in a decrease in the stiffness of the AFG CNTRC nanobeams, consequently leading to an increase in dimensionless deflection.

• In contrast to the nonlocality effect, dimensionless deflections decrease as the length scale parameter λ increases.

In conclusion, the structure presented in this study offers benchmark results that can be utilized in the design of composite structures. Moreover, the proposed solution method can be subject to future comparisons with other approximate methods, including the finite-element method.

References

Abdelhaffez, G.S., Daikh, A.A., Saleem, H.A. and Eltaher, M.A. (2023), "Buckling analysis of coated functionally graded spherical nanoshells resting on an orthotropic elastic medium", *Mathematics*, **11**(2), 409. https://doi.org/10.3390/math11020409

Abdelrahman, A.A. and Eltaher, M.A. (2020), "On bending and buckling responses of perforated nanobeams including surface energy for different beams theories", *Eng. Comput.*, 1-27. https://doi.org/10.1007/s00366-020-01211-8

Abo-bakr, H.M., Abo-bakr, R.M., Mohamed, S.A. and Eltaher, M.A. (2021), "Multi-objective shape optimization for axially

functionally graded microbeams", *Compos. Struct.*, **258**, 113370. https://doi.org/10.1016/j.compstruct.2020.113370

Abo-Bakr, R.M., Eltaher, M. A. and Attia, M.A. (2020), "Pull-in and freestanding instability of actuated functionally graded nanobeams including surface and stiffening effects", *Eng. Comput.*, 1-22. https://doi.org/10.1007/s00366-020-01146-0

Akgoz, B., (2019), "Static stability analysis of axially functionally graded tapered micro columns with different boundary conditions", *Steel Compos. Struct.*, **33**(1), 133-142. http://doi.org/10.12989/scs.2019.33.1.133

Askes, H. and Aifantis, E.C. (2009), "Gradient elasticity and flexural wave dispersion in carbon nanotubes", *Phys. Rev. B*, **80**(19), 195412. https://doi.org/10.1103/PhysRevB.80.195412

Bekhadda, A., Cheikh, A., Bensaid, I., Hadjoui, A. and and Daikh, A. (2019), "A novel first order refined shear-deformation beam theory for vibration and buckling analysis of continuously graded beams", *Adv. Aircr. Spacecr. Sci.*, **6**(3), 189-206. https://doi.org/10.12989/aas.2019.6.3.189

Belarbi, M.O. and Tati, A. (2016), "Bending analysis of composite sandwich plates with laminated face sheets: New finite element formulation", *J. Solid Mech.*, **8**(2), 280-299.

Belarbi, M.O., Houari, M.S.A. Daikh, A.A. Garg, A. Merzouki, T. Chalak, H.D. and Hirane, H. (2021), "Nonlocal finite element model for the bending and buckling analysis of functionally graded nanobeams using a novel shear deformation theory", *Compos. Struct.*, **264**, 113712. https://doi.org/10.1016/j.compstruct.2021.113712

Bensaid, I., Daikh, A.A. and Drai, A. (2019), "Size-dependent free vibration and buckling analysis of sigmoid and power law functionally graded sandwich nanobeams with microstructural defects", *Proc IMechE Part C J Mech. Eng. Sci.*, **234**(18), 3667-3688. https://doi.org/10.1177/0954406220916481

Cao, D., Gao, Y. Yao, M.and Zhang, W. (2018), "Free vibration of axially functionally graded beams using the asymptotic development method", *Eng. Struct.*, **173**, 442-448. https://doi.org/10.1016/j.engstruct.2018.06.111

Civalek, Ö., Dastjerdi, S., Akbaş Ş. and Akgöz B. (2021), "Vibration analysis of carbon nanotube-reinforced composite microbeams", *Math. Meth. Appl. Sci.*, Special Issue Paper. https://doi.org/10.1002/mma.7069

Daikh, A.A., Bensaid, I., Bachiri, A., Houari, M.S.A. Tounsi, A. and Merzouki, T. (2020d), "On static bending of multilayered carbon nanotube-reinforced composite plates", *Comput. Concr.*, **26**(2). https://doi.org/10.12989/cac.2020.26.2.000

Daikh, A.A. (2019), "Temperature dependent vibration analysis of functionally graded sandwich plates resting on Winkler/ Pasternak/Kerr foundation", *Mater. Res. Express*, **6**. 065702. https://doi.org/10.1088/2053-1591/ab097b

Daikh, A.A. and A.M. Zenkour, (2020), "Bending of functionally graded sandwich nanoplates resting on pasternak foundation under different boundary conditions", *J. Appl. Comput. Mech.*, 2020. https://doi.org/10.22055/JACM.2020.33136.2166

Daikh, A.A. and Zenkour, A.M. (2019a), "Free vibration and buckling of porous power-law and sigmoid functionally graded sandwich plates using a simple higher-order shear deformation theory", *Mater. Res. Express*, 6115707. https://doi.org/10.1088/2053-1591/ab48a9

Daikh, A.A. and Zenkour, A.M. (2019), "Effect of porosity on the bending analysis of various functionally graded sandwich plates", *Mater Res Express*, **6**, 065703. https://doi.org/10.1088/2053-1591/ab0971

Daikh, A.A. and Zenkour, A.M. (2020), "Bending of functionally graded sandwich nanoplates resting on Pasternak foundation under different boundary conditions", *J. Appl. Comput. Mech.*, **6**, 1245-1259. https://doi.org/10.22055/JACM.2020.33136.2166

Daikh, A.A., Houari, M.S.A., Belarbi, M.O., Chakraverty, S. and Eltaher, M.A. (2021a), "Analysis of axially temperature dependent functionally graded carbon nanotube reinforced composite plates", *Eng. Comput.*, **38**(Suppl 3), 2533-2554. https://doi.org/10.1007/s00366-021-01413-8

Daikh, A.A., A. Drai, M.S.A. Houari, and Eltaher, M.A. (2020f), "Static analysis of multilayer nonlocal strain gradient nanobeam reinforced by carbon nanotubes", *Steel Compos. Struct.*, **36**(6), 643-656. http://dx.doi.org/10.12989/scs.2020.36.6.643

Daikh, A.A., Bachiri, A., Houari, M.S.A. and Tounsi, A. (2020b), "Size dependent free vibration and buckling of multilayered carbon nanotubes reinforced composite nanoplates in thermal environment", *Mech. Based Des. Struct.*, 1-29. https://doi.org/10.1080/15397734.2020.1752232

Daikh, A.A., Bensaid, I and Zenkour, A.M. (2020d), "Temperature dependent thermomechanical bending response of functionally graded sandwich plates", *Eng. Res. Express*, **2**, 015006. https://doi.org/10.1088/2631-8695/ab638c

Daikh, A.A., Drai, A. Bensaid, I. Houari, M.S.A. and Tounsi, A. (2020a), "On vibration of functionally graded sandwich nanoplates in the thermal environment", *J. Sandw. Struct. Mater.*, **23**(6), 2217-2244. https://doi.org/10.1177/1099636220909790

Daikh, A.A., Guerroudj, M., Elajrami, M., Megueni, A., (2019a), "Thermal buckling of functionally graded sandwich beams", *Adv. Mater. Res.*, **1156**, 43-59. https://doi.org/10.4028/www.scientific.net/AMR.1156.43

Daikh, A.A., Houari, M.S.A. and Eltaher, M.A. (2020c), "A novel nonlocal strain gradient Quasi-3D bending analysis of sigmoid functionally graded sandwich nanoplates", *Compos. Struct.*, 113347. https://doi.org/10.1016/j.compstruct.2020.113347

Daikh, A.A., Houari, M.S.A., Karami, B., Eltaher, M.A., Dimitri, R. and Tornabene, F. (2021b), "Buckling analysis of CNTRC curved sandwich nanobeams in thermal Environment", *Appl. Sci.*, **11**, 3250. https://doi.org/10.3390/app11073250

Daikh, A.A., Houari, M.S.A., Tounsi, A. (2019b), "Buckling analysis of porous FGM sandwich nanoplates due to heat conduction via nonlocal strain gradient theory", *Eng. Res. Express*, **1**, 015022. https://doi.org/10.1088/2631-8695/ab38f9

Ebrahimi, F. and Barati, M.R. (2018), "Buckling analysis of nonlocal strain gradient axially functionally graded nanobeams resting on variable elastic medium", *Proceedings of the Institution of Mechanical Engineers, Part C: Journal of Mechanical Engineering Science*, **232**(11), 2067-2078. https://doi.org/10.1177/0954406217713518

El-Ashmawy, A.M. and Xu, Y. (2021), "Combined effect of carbon nanotubes distribution and orientation on functionally graded nanocomposite beams using finite element analysis", *Mater. Res. Express*, **8**(1), 015012. https://doi.org/10.1088/2053-1591/abc773

Eltaher, M.A. and Mohamed, N. (2020a), "Nonlinear stability and vibration of imperfect CNTs by doublet mechanics", *Appl. Math. Comput.*, **382**, 125311. https://doi.org/10.1016/j.amc.2020.125311

Eltaher, M.A., El-Borgi, S. and Reddy, J.N. (2016), "Nonlinear analysis of size-dependent and material-dependent nonlocal CNTs", *Compos. Struct.*, **153**, 902-913. https://doi.org/10.1016/j.compstruct.2016.07.013

Eringen, A.C. (1972), "Nonlocal polar elastic continua", *International Journal of Engineering Science*, **10**(1): 1-16. https://doi.org/10.1016/0020-7225(72)90070-5

Eringen, A.C. (1983), "On differential equations of nonlocal elasticity and solutions of screw dislocation and surface waves", *J. Appl. Phys.*, **54**(9), 4703-4710. https://doi.org/10.1063/1.332803

Esen, I., Özarpa, C. and Eltaher, M.A. (2021), "Free vibration of a cracked FG microbeam embedded in an elastic matrix and exposed to magnetic field in a thermal environment", *Compos. Struct.*, **261**, 113552. https://doi.org/10.1016/j.compstruct.2021.113552

Ferreira, A., Castro, L.M. and Bertoluzza, S. (2009), "A high order collocation method for the static and vibration analysis of composite plates using a first-order theory", *Compos. Struct.*, **89**(3), 424-432. https://doi.org/10.1016/j.compstruct.2008.09.006

Ghannadpour, S., Mohammadi, B. and Fazilati, J. (2013), "Bending, buckling and vibration problems of nonlocal Euler beams using Ritz method" *Compos. Struct.*, **96**, 584-589. https://doi.org/10.1016/j.compstruct.2012.08.024

Hamed, M.A., Abo-bakr, R.M., Mohamed, S.A. and Eltaher, M.A. (2020), "Influence of axial load function and optimization on static stability of sandwich functionally graded beams with porous core", *Eng. Comput.*, **36**(4), 1929-1946. https://doi.org/10.1007/s00366-020-01023-w

Houari, M.S.A., Bessaim, A. Bernard, F. Tounsi, A. and Mahmoud, S.R. (2018), "Buckling analysis of new quasi-3D FG nanobeams based on nonlocal strain gradient elasticity theory and variable length scale parameter", *Steel Compos. Struct.*, **28**(1),13-24. http://dx.doi.org/10.12989/scs.2018.28.1.013

Karamanli, A. and Vo, T.P. (2021), "Finite element model for carbon nanotube-reinforced and graphene nanoplatelet-reinforced composite beams", *Compos. Struct.*, **264**, 113739. https://doi.org/10.1016/j.compstruct.2021.113739

Karamanli, A., Eltaher, M.A., Thai, S. and Vo, T.P. (2023). "Transient dynamics of 2D-FG porous microplates under moving loads using a higher-order finite element model", *Eng. Struct.*, **278**, 115566. https://doi.org/10.1016/j.engstruct.2022.115566

Khaniki, H.B. and Ghayesh, M.H. (2020), "On the dynamics of axially functionally graded CNT strengthened deformable beams", *Eur. Phys. J. Plus*, **135**(5), 415. https://doi.org/10.1140/epjp/s13360-020-00433-5

Li, X., Li, L. Hu, Y. Ding, Z. and Deng, W. (2017), "Bending, buckling and vibration of axially functionally graded beams based on nonlocal strain gradient theory", *Compos. Struct.*, **165**, 250-265. https://doi.org/10.1016/j.compstruct.2017.01.032

Lim, C.W., Zhang, G. and Redd, J.N. (2015), "A higher-order nonlocal elasticity and strain gradient theory and its applications in wave propagation", *J. Mech. Phys. Solids*, **78**, 298-313. https://doi.org/10.1016/j.jmps.2015.02.001

Mehrabadi, S.J., Aragh, B.S., Khoshkhahesh, V. and Taherpour, A. (2012), "Mechanical buckling of nanocomposite rectangular plates reinforced by aligned and straight single-walled carbon nanotubes", *Compos. Part B Eng.*, **43**(4), 2031-2040. https://doi.org/10.1016/j.compositesb.2012.01.067

Mindlin, R.D. (1963), "Microstructure in linear elasticity", Columbia Univ New York, Dept of Civil Engineering and Engineering Mechanics. https://doi.org/10.1007/BF00248490

Mohamed, N., Mohamed, S.A. and Eltaher, M.A. (2020), "Buckling and post-buckling behaviors of higher order carbon nanotubes using energy-equivalent model", *Eng. Comput.*, 1-14. https://doi.org/10.1007/s00366-020-00976-2

Nejad, M.Z., Hadi, A. Omidvari, A. and Rastgoo, A. (2018), "Bending analysis of bi-directional functionally graded Euler-Bernoulli nano-beams using integral form of Eringen's non-local elasticity theory", *Struct. Eng. Mech.*, **67**(4), 417-425. https://doi.org/10.12989/sem.2018.67.4.417

Nguyen, V.H., Nguyen, T.K. Thai, H.T. and Vo, T.P. (2014), "A new inverse trigonometric shear deformation theory for isotropic and functionally graded sandwich plates", *Compos. Part B Eng.*, **66**, 233-246. https://doi.org/10.1016/j.compositesb.2014.05.012

Rajasekaran, S. and Bakhshi Khaniki, H. (2019), "Finite element static and dynamic analysis of axially functionally graded nonuniform small-scale beams based on nonlocal strain gradient theory", *Mech. Adv. Mater. Struct.*, **26**(14), 1245-1259. https://doi.org/10.1080/15376494.2018.1432797

Sarkar, K. and Ganguli, R. (2014), "Closed-form solutions for axially functionally graded Timoshenko beams having uniform cross-section and fixed–fixed boundary condition", *Compos. Part B Eng.*, **58**, 361-370. https://doi.org/10.1016/j.compositesb.2013.10.077

Shafiei, N., Kazemi, M. Safi, M. and Ghadiri, M. (2016), "Nonlinear vibration of axially functionally graded non-uniform nanobeams", *Int. J. Eng. Sci.*, **106**, 77-94. https://doi.org/10.1016/j.ijengsci.2016.05.009

Shen, H.S., (2009), "Nonlinear bending of functionally graded carbon nanotube-reinforced composite plates in thermal environments", *Compos. Struct.*, **91**(1), 9-19. https://doi.org/10.1016/j.compstruct.2009.04.026

Shen, H.S., He, X.Q. and Yang, D.Q. (2017), "Vibration of thermally postbuckled carbon nanotube-reinforced composite beams resting on elastic foundations", *Int. J. Non-Linear Mech.*, **91**, 69-75. https://doi.org/10.1016/j.ijnonlinmec.2017.02.010

Şimşek, M. (2015), "Size dependent nonlinear free vibration of an axially functionally graded (AFG) microbeam using He's variational method", *Compos. Struct.*, **131**, 207-214. https://doi.org/10.1016/j.compstruct.2015.05.004

Thai, C.H., Zenkour, A. Wahab, M.A. and Nguyen-Xuan, H. (2016), "A simple four-unknown shear and normal deformations theory for functionally graded isotropic and sandwich plates based on isogeometric analysis", *Compos. Struct.*, **139**, 77-95. https://doi.org/10.1016/j.compstruct.2015.11.066

Tornabene, F., Bacciocchi, M., Fantuzzi, N. and Reddy, J. N. (2019). "A multiscale approach for Three-Phase CNT/Polymer/ Fiber laminated nanocomposite structures", *Polym. Compos.*, **40**, 102-126. https://doi.org/10.1002/pc.24520

Vo, T.P., Thai, H.T. Nguyen, T.K. Inam, F.and Lee, J. (2015), "A quasi-3D theory for vibration and buckling of functionally graded sandwich beams", *Compos. Struct.*, **119**, 1-12. https://doi.org/10.1016/j.compstruct.2014.08.006

Wang, Y. and Wu, D. (2016), "Thermal effect on the dynamic response of axially functionally graded beam subjected to a moving harmonic load", *Acta Astronautica*, **127**, 171-181. https://doi.org/10.1016/j.actaastro.2016.05.030

Wang, Y., Ren, H. Fu, T.and Shi, C. (2020), "Hygrothermal mechanical behaviors of axially functionally graded micro-beams using a refined first order shear deformation theory", *Acta Astronautica*, **166**, 306-316. https://doi.org/10.1016/j.actaastro.2019.10.036

Wattanasakulpong, N. and Ungbhakorn, V. (2013), "Analytical solutions for bending, buckling and vibration responses of carbon nanotube-reinforced composite beams resting on elastic foundation", *Comput. Mater. Sci.*, **71**, 201-208. http://doi.org/10.1016/j.commatsci.2013.01.028

Yang, F., Chong, A., Lam, D.C.C. and Tong, P. (2002), "Couple stress based strain gradient theory for elasticity", *Int. J. Solids Struct.*, **39**(10), 2731-2743. https://doi.org/10.1016/S0020-7683(02)00152-X

Zenkour, A. and Radwan, A. (2020), "Bending and buckling analysis of FGM plates resting on elastic foundations in hygrothermal environment", *Arch. Civil Mech. Eng.*, **20**(4), 1-23. https://doi.org/10.1007/s43452-020-00116-z

Zhen, Y.X., Wen, S.L. and Tang, Y. (2019), "Free vibration analysis of viscoelastic nanotubes under longitudinal magnetic field based on nonlocal strain gradient Timoshenko beam model", *Physica E*, **105**, 116-124**.** https://doi.org/10.1016/j.physe.2018.09.005

AT